ESS505 Term Project: A Method to Track Temporal Changes in SWE on a Glacier Using InSAR

Eric Gagliano

Term Paper Format

The final paper should be the format, style, and length equivalent of a publication in Geophysical Research Letters or Geology. Both journals aim to rapidly publish short-format, high-impact research of interdisciplinary interest. Paper length should be approximately 2000 to 2500 words (∼4 formatted pages), including the abstract (250 words or less), but excluding figure/table captions, citations, and references. Approximately four display items (figures or tables) can be included. No more than 30 references should be cited. If data and/or new computational methods are presented in the paper, information on data/computational code availability should be given. Supplements/appendices can be used to further explain mathematical or other background information and allow presentation of additional data, but the paper should be written such that this information is truly supplemental and is not essential to understand the main conclusions. Both Geology and Geophysical Research Letters provide manuscript templates to aid in formatting.

Key Points:

- Using glacier velocity estimates and InSAR, we created a method to track temporal changes in SWE on glaciers and applied our approach to South Cascade Glacier.

Corresponding author: Eric Gagliano, egagli@uw.edu

Abstract

This paper describes an approach to mapping changes in snow water equivalent (SWE) using Interferometric Synthetic Aperture Radar (InSAR) on a glacier. Between the two dates of an interferogram, we can isolate the change in interferometric phase due to changes in SWE by minimizing all other interferogram phase contributions. Unique to this study, we estimate the velocity of a glacier and simulate the change in interferometric phase we would expect due to glacier motion. Subtracting this phase contribution, we are left with a change in interferometric phase which we can directly relate to change in SWE between the two interferogram dates. To test our approach, we build interferograms from Sentinel-1 SAR data, estimate glacier velocities from ITS_LIVE data, and finally produce estimates for change in SWE over South Cascade Glacier.

Plain Language Summary

We developed a new method to measure the amount of snow on top of a glacier using speed measurements of the glacier and a special type of radar attached to a satellite. The speed measurements help us figure out how far the glacier has moved between two different times. The radar produces waves that move differently in snow than in air, so by taking multiple radar measurements over the same location at different times and combining this data with our speed measurements, we can track the change in amount of snow on the glacier over time. Knowing the amount of snow on top of a glacier will help us better understand how the mass of a glacier changes over time, will help us estimate how much light will be reflected off of the glacier, and is also helpful for managing the water that drains from the glacier.

1 Introduction

1.1 Snow Water Equivalent

Snow water equivalent (SWE) quantifies the amount of water in snowpack. SWE is important to know for water resource mangement, flood prediction, and various surface parameters such as albedo and ground/soil insulation from temperature changes. Traditionally, SWE has been measured using in situ methods. In situ methods include digging snow pits and also placing "snow pillows" which measure the weight of water. In situ data is not well geographically distributed nor is it consistently taken (Robinson et al., 1993). Methods of obtaining SWE have been changing with the improvement of many remote sensing methods that utilize optical and SAR imagery, altimetry data, etc (Tedesco et al., 2015).

1.2 Interferometric Synthetic Aperture Radar

Interferometric Synthetic Aperture Radar (InSAR) is a remote sensing technology that measures the phase difference between two consecutive Synthetic Aperature Radar (SAR) images of a location. InSAR is a great tool for measuring very small changes from space, and is commonly used to detect small changes in subsidence, volcano deformations, hazards such as earthquakes and landslides, and in glaciologic applications like measuring glacial velocities and mapping grounding lines. The contributions to the phase of a SAR image are:

$$\phi = \phi_{flat} + \phi_{topography} + \phi_{deformation} + \phi_{atmosphere} + \phi_{orbit} + \phi_{noise}$$

Where ϕ_{flat} is the phase contribution due to look angles and projections to the ground, $\phi_{topography}$ is the phase contribution due to topography, $\phi_{deformation}$ is the phase contribution due to changes in range distance from one measurement to the next, $\phi_{atmosphere}$ is the phase contribution due to atmospheric effects (mainly water vapor), ϕ_{orbit} is the phase contribution due to orbital position and associated errors, and ϕ_{noise} is the phase contribu-

tion due to noise (Deeb, 2012). While there are other types of InSAR, this paper focuses on repeat pass interferometry so we can measure the phase difference between two SAR images taken over the same location at different times. This phase difference is represented as an interferogram.

1.3 Extracting Changes in SWE using InSAR

Guneriussen et al. (2001) first describes a method for extracting changes in SWE (ΔSWE) by relating ΔSWE to change in interferoemtric phase. Due to the dielectric contrast between the air and snow, the radar beam vector is refracted and appears to have a shorter range distance due to this geometric distortion as seen in Figure 1. Thus, a shorter range distance corresponds to higher ΔSWE. More precisely, the authors relate the change in interferometric phase due to snow $\Delta\phi_{snow}$ to change in snow depth Δz_{snow}, dielectric constant of snow ϵ, incidence angle θ_i, and wavelength λ in the following equation:

$$\Delta\phi_{snow} = \frac{-4\pi}{\lambda}\Delta z_{snow}(\cos\theta_i - \sqrt{\epsilon - \sin\theta_i^2})$$

where the dielectric constant of snow: ϵ is related to snow density by:

$$\epsilon = 1 + 1.6\rho_{snow} + 1.8\rho_{snow}^3$$

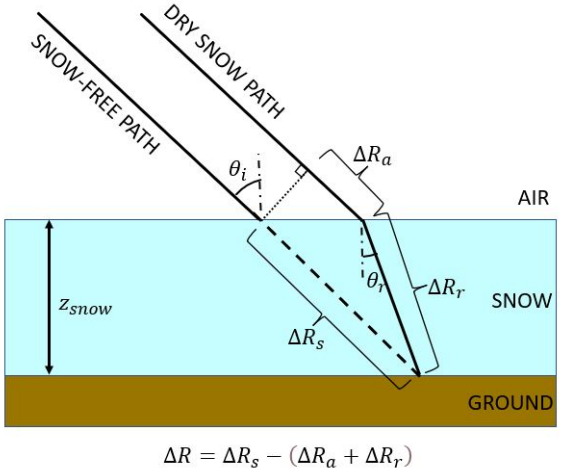

Figure 1. Change in Range Distance ΔR. Figure adapted from (Guneriussen et al., 2001).

Previous studies such as Conde et al. (2019) have successfully used Sentinel-1 C-band SAR data to measure ΔSWE over a period of 6 days with a resolution of 20m and sub-centimeter ΔSWE accuracy. Novel about this study was their use of a numerical weather model in order to minimize the change in interferometric phase from the atmosphere. However, this study also assumes no change in interferometric phase due to terrain deformation or motion.

1.4 Goal: Using InSAR to Extract ΔSWE in Areas with Deformation/Motion

Previously, InSAR has proven effective in detecting ΔSWE in areas where the terrain deformation/motion is assumed to be zero. In this paper, we intend to extend the limits of detecting ΔSWE using InSAR by attempting to measure ΔSWE over areas with significant glacial motion.

2 Methods

2.1 The Game Plan

Isolating ΔSWE becomes a lot harder on a glacier due to glacier motion contributing to a change in interferometric phase. In order to capture both glacial motion and ΔSWE, we split up interferometric phase change from changes in range distance into two different variables, change from deformation (which will model our glacial motion) $\Delta\phi_{deformation}$, and $\Delta\phi_{snow}$ which represents ΔSWE. (We split this term into a true deformation component and a snow component because while they both correspond to a change in interferometric phase due to a change in range distance, they are produced by different phenomena and change independently of each other). Therefore, through the rest of this paper, we will continue to use "deformation" to mean glacier motion. Accordingly, the equation for interferometric phase change in an interferogram is:

$$\Delta\phi_{interferogram} = \frac{4\pi}{\lambda}\frac{B_\perp}{R\sin\theta}h_{error} + \frac{4\pi}{\lambda}\nu\Delta t + \Delta\phi_{atmosphere} + \Delta\phi_{snow} + \Delta\phi_{noise}$$

In this representation, $\frac{4\pi}{\lambda}\frac{B_\perp}{R\sin\theta}h_{error}$ corresponds to $\Delta\phi_{topography}$ and $\frac{4\pi}{\lambda}\nu\Delta t$ corresponds to $\Delta\phi_{deformation}$. We will work to minimize all terms except for $\Delta\phi_{snow}$ in order to recover ΔSWE.

2.2 Modeling Phase Contribution Due to Glacier Motion

In order to remove this phase contribution due to glacier motion, we could either take a displacement or velocity approach. The displacement approach would require two Digital Elevation Models (DEM)s acquired at the same time as each image in the interferogram pair. We would then project the DEMs into the radar geometry, difference them, and convert this elevation difference into a simulated change in interferometric phase.

$$\Delta\phi_{deformation} = \frac{4\pi}{\lambda}\nu\Delta t$$

where

$$\nu\Delta t = \Delta DEM_{LineOfSight(LOS)}$$

The velocity approach would assume a constant velocity estimate over the temporal baseline of the interferometric pair which we would then multiply by the temporal baseline to recover the change in position of the glacier. With this change in position, we would again convert this elevation difference into a simulated change in interferometric phase.

$$\Delta\phi_{deformation} = \frac{4\pi}{\lambda}\nu_{LOS}\Delta t$$

where ν_{LOS} is the average velocity in the line of sight direction and Δt is the time between the interferogram pair.

We decided to settle on the velocity approach because of the difficulty in obtaining DEMs that were created at the same time as the interferogram pair. We chose to use ITS_LIVE velocity data from JPL because of ease of accessibility (Gardner et al., 2019). However, this data has many flaws. The data is only in the x and y directions, so we must make the assumption that flow is parallel to the bed. The data we retrieved is averaged over a year, so it is not a good representation of velocity on a smaller time scale. The data is also bad in terms of accuracy as we will soon see...

2.3 The Rest of the Terms

While the change in interferometric phase due to the glacier motion term and the ΔSWE term are expected to dominate, it's important to briefly mention the rest of the

terms and their affect on our calculations. The $\frac{4\pi}{\lambda}\frac{B_\perp}{R\sin\theta}h_{error}$ (a.k.a. $\Delta\phi_{topography}$) term is easily minimized by choosing a small spatial baseline $B_\perp$ for our interferometric pair and also by having a reasonably accurate DEM for topographic corrections. Therefore, we will choose an interferometric pair with a $B_\perp$ of $< 50m$ and use a $30m$ DEM. The $\Delta\phi_{atmosphere}$ term will be minimized by choosing a small temporal baseline between the interferometric pair. However, this can be handled much more effectively by using a Numerical Weather Model (Conde et al., 2019). However, Rott et al. (2003) found that ignoring atmospheric effects is still viable because a requirement for ΔSWE retrieval via InSAR is that the snow must be dry, and when snow is dry that also means atmospheric temperatures and water vapor content should be low, reducing the importance of the atmospheric term. For our purposes the $\Delta\phi_{noise}$ term should both be negligible (Majumdar, 2019).

2.4 Interferograms & Data Processing

First, we selected the interferometric pairs through ASF's Data Search Vertex site. We focused on images with descending orbits during the accumulation season. To create the interferograms, we fed our granule selections into ASF's HyP3 One-Time Processing pipeline. This pipeline uses GAMMA's InSAR software to create the interferograms. Once the interferogram is collected, we crop and warp our interferogram and the ITS_LIVE velocity data to our area of interest. We simulate the corresponding $\Delta\phi_{deformation}$ for each pixel's velocity in the line of sight direction. Next, we retrieve our change in interferometric phase due to ΔSWE: $\Delta\phi_{interferogram} - \Delta\phi_{deformation} = \Delta\phi_{snow}$ After we have isolated $\Delta\phi_{snow}$, we simply combine the relations:

$$\Delta\phi_{snow} = \frac{-4\pi}{\lambda}\Delta z_{snow}(\cos\theta_i - \sqrt{\epsilon - \sin\theta_i^2}) \quad \epsilon = 1 + 1.6\rho_{snow} + 1.8\rho_{snow}^3 \quad \Delta\text{SWE} = \frac{\rho_{snow}}{\rho_{water}}\Delta z_{snow}$$

$$\text{for a final } \Delta \text{ SWE of: } \Delta\text{SWE} = \frac{\lambda}{2\pi}\frac{1}{\alpha(1.59 + \theta_i^{\frac{5}{2}})}\Delta\phi_{snow} \quad \text{(Conde et al., 2019)}$$

where $\alpha = 1$ (Leinss et al., 2015). After performing this equation on each pixel's $\Delta\phi_{snow}$ estimate, the resulting product is a ΔSWE map.

2.5 Study Area

The area we chose to study was South Cascade Glacier (SCG). We chose this area because it is well studied and thus has relatively well known properties (Krimmel, 2001). See Figure 2.

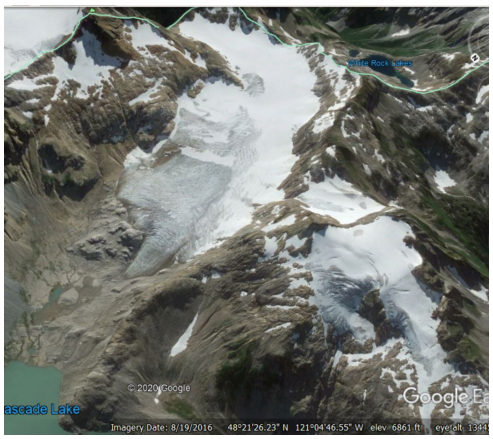

Figure 2. Google Earth Image of South Cascade Glacier

2.6 What We Expect: Relative Magnitudes of $\Delta\phi_{snow}$ & $\Delta\phi_{deformation}$

Important to our ability to measure ΔSWE is our ability to separate $\Delta\phi_{snow}$ from $\Delta\phi_{deformation}$. In order to see the relative magnitudes of both of these changes in interferometric phase, we constructed the theoretical plot in Figure 3.

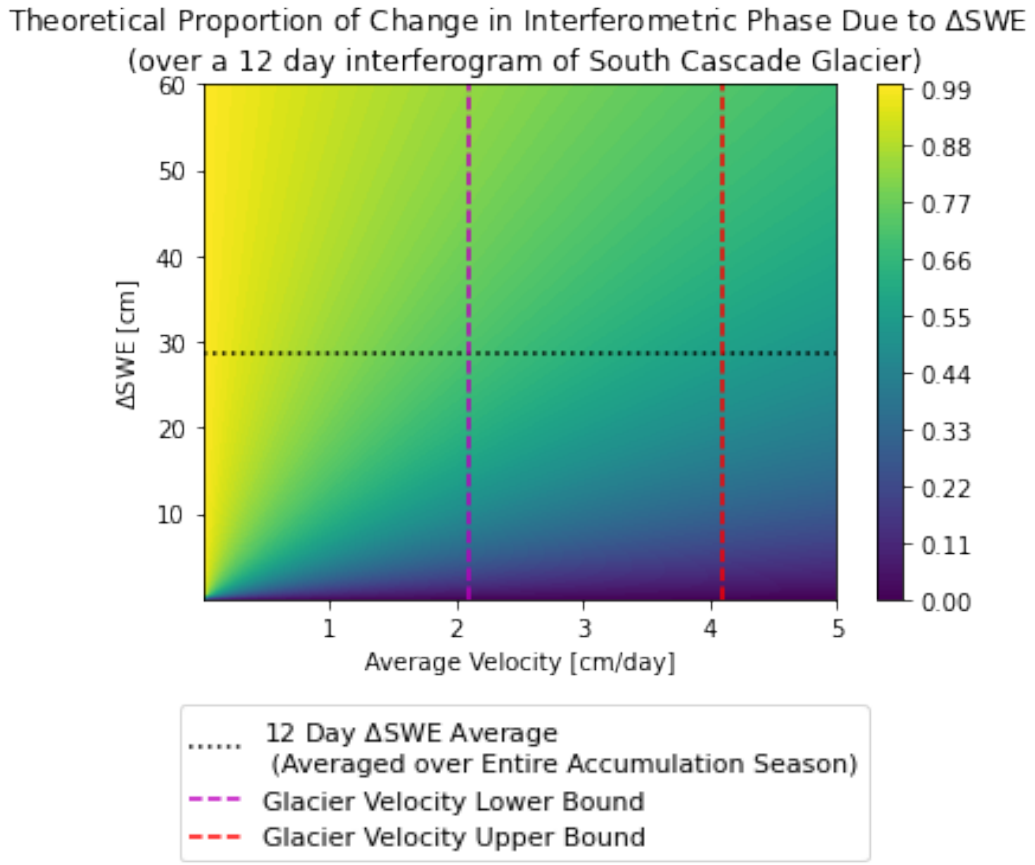

Figure 3. Proportion of Change in Interferometric Phase due to ΔSWE

This theoretical plot shows how the proportion

$$\frac{\Delta\phi_{snow}}{\Delta\phi_{snow} + \Delta\phi_{deformation}}$$

varies at different values of glacier velocity and ΔSWE over a period of 12 days. The purple and red dashed vertical lines bound usual average glacier velocities for SCG in the accumulation season, and the black dotted horizontal line shows the average ΔSWE we would expect over the 12 day period. It's important to keep in mind though that while glacier velocities should hold relatively constant over the 12 day period, ΔSWE can vary wildy. There could easily be interferogram periods where there is zero snowfall, and interferogram periods with much higher than average snowfall. This plot shows us that given accurate velocity information, it should be possible to tease out the ΔSWE signal because both are of similar magnitudes in the corridor of usual average velocities. In fact, at the season averaged value of ΔSWE, we would expect half of the change in interferometric phase to be attributed to the glacier velocity, and half attributed to ΔSWE.

3 Results

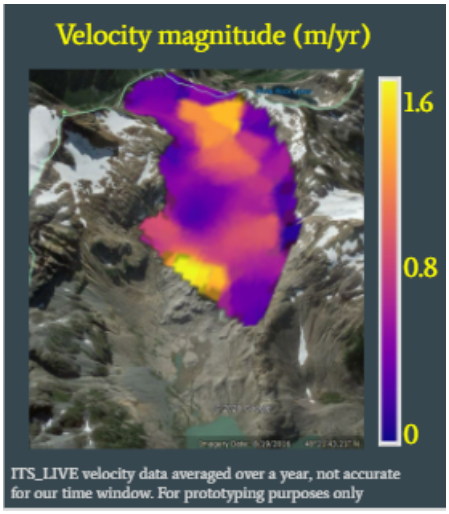

Figure 4. Velocity Magnitude Data from ITS_LIVE

First, we visualized our ITS_LIVE velocity data in Figure 4. This looks pretty bad, with a maximum value of 1.6m/yr (which is much slower than expected!) but it's all we have to use for the velocity for now.

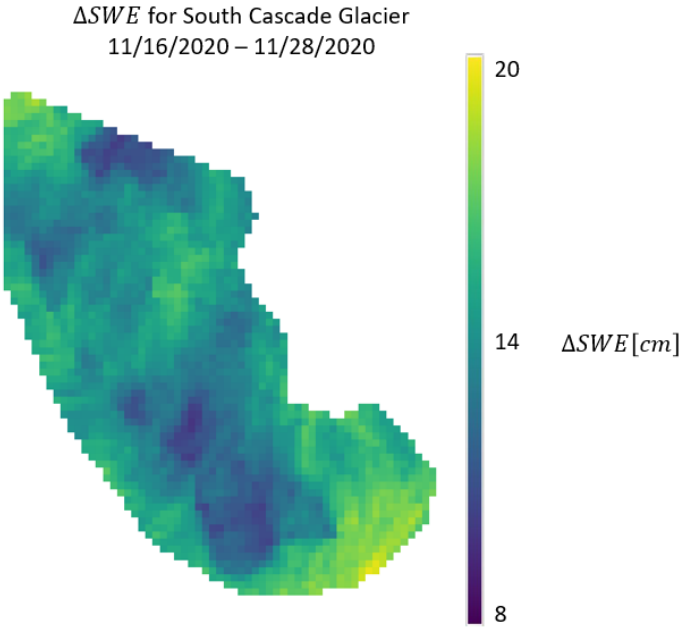

Figure 5. ΔSWE On South Cascade Glacier from 11/16/2020 - 11/28/2020

As visualized in Figure 5, our minimum ΔSWE value was about 9 cm, and our maximum value was about 19.5 cm. The glacier-wide average ΔSWE value was 14.27 cm. The higher ΔSWE values seem to be at the top of the glacier and along the edges. We provide the following Figure 6 for more context.

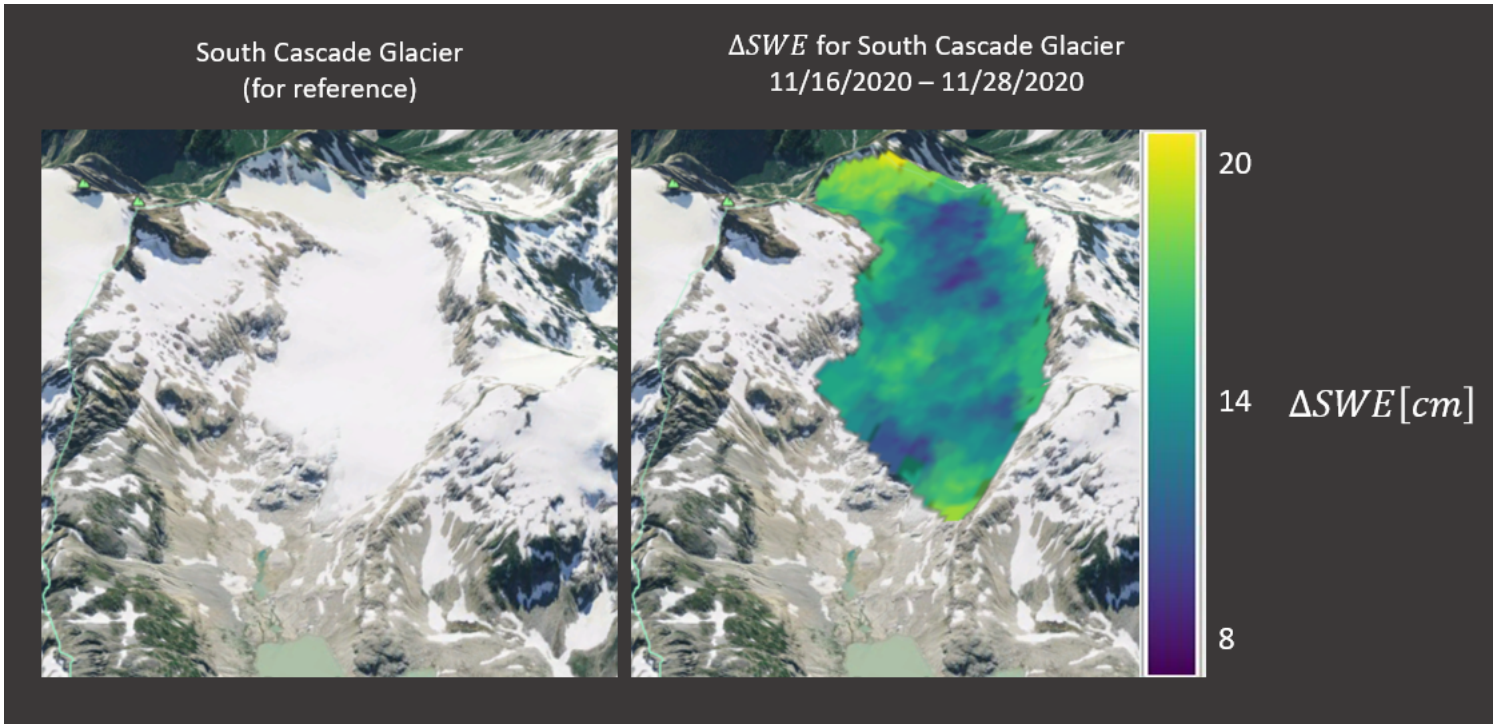

Figure 6. ΔSWE On South Cascade Glacier from 11/16/2020 - 11/28/2020 (with context)

4 Discussion/Conclusion

4.1 Initial Impressions

At first glance, these results are coarse and flawed. Just by inspection, we note that our input velocity data from ITS_LIVE is off by an order of magnitude and our ΔSWE could be a bit low. Fortunately, we have a good idea of why our results are bad, and we can work on improving them in the future. We discuss these errors and possible improvements in subsections 4.3-4.5. Regardless, this project has allowed us to establish a basic workflow to extract ΔSWE once we have good interferometric and velocity input data.

4.2 Comparing to Real Data

It is hard to compare our results to real SWE data since InSAR measures ΔSWE and not absolute SWE. Most publicly available SWE measurements don't have the temporal resolution to evaluate ΔSWE over the small time spans of our 12 day interferogram pairs. Plus, ΔSWE is highly variable over time. So, for a very rough comparison we looked at the ΔSWE value over the entire accumulation season and recovered a weekly average ΔSWE as suggested by Knut. Knut notes that on the higher parts of SCG, winter balance is about 5m water equivalent. Other sources seemed to suggest similar values, with an average somewhere between 2-5m of water equivalent. Our top bound for a 12 day interferogram period would correspond to a ΔSWE of 30cm, though for the entire glacier we might expect a lower value. This actually corresponds nicely with our calculated average ΔSWE value of 14.27cm during the 11/16/2020 - 11/28/2020 period at SCG. However, due to our input velocity values being lower than the likely correct value, this error would propogate and end up lowering our calculated ΔSWE values. Thus, we would expect to undershoot ΔSWE values if we had correct velocity data.

4.3 Issue 1: Bad Velocity Data

First, our velocities are extremely low: likely an order of magnitude lower than expected. Also, we notice the velocity magnitude and ΔSWE graphs look eerily similar. This confirms what we learned from our theoretical calculations in Figure 3, that our interferograms will mostly contain velocity data as opposed to ΔSWE data. Thus, our ΔSWE calculation is very sensitive to our velocity input data, and our faulty ITS_LIVE annually averaged data is insufficient in properly constraining the phase contribution due to glacier velocity.

4.4 Issue 2: Lack of Interferometric Coherence

The main barrier to good results is the lack of coherence we get in our interferograms. This is likely because of the geometry of our study area, heterogeneity in the spatial distribution of ΔSWE, and the 12 day revisit time, among other factors. Coherence in this context can be thought of as nearby pixels behaving similarly in terms of their change in phase. See the Possible Improvements subsection for more details.

4.5 Possible Improvements

Here we note seven main routes to explore for improving future results.

4.5.1 Study Area

Find a better study area. This area should have less complicated surrounding geography. This area should have SAR image pairs with better coherence to improve interferogram

correlation. A location with a higher revisit time should be chosen. Sentinel-1 has a revisit time of 12 days over SCG, wheras areas such as Finland have a revisit time of 6 days.

4.5.2 L-Band Data

To increase coherence, we can try exploring applying our method to L-band data. This will produce results with less precise ΔSWE values, though they will overall be more accurate because of the higher coherence with snow cover of L-band SAR. If we can apply our method to L-band data, we could potentially leverage the capabilities of the upcoming NISAR mission.

4.5.3 Improved Velocity/Displacement Data

In order for our method to calculate ΔSWE by isolating $\Delta\phi_{snow}$, we must be able to remove the change in interferometric phase due to glacier motion $\Delta\phi_{deformation}$. This requires well constrained velocity or displacement data, not the inaccurate and coarse estimates used in this study. See Figure 3 for expected relative change in interferometric phase contributions given an estimated velocity range.

4.5.4 Numerical Weather Model

We can use a Numerical Weather Model to reduce the influence of $\Delta\phi\_atmosphere$ in our $\Delta\phi_{snow}$ calculations (Conde et al., 2019).

4.5.5 Interferogram Processing

ASF's HyP3 processing pipeline was great for ease of use, but we quickly ran out of processing credits. In order to process as many interferograms as we want and also have better control over the process, we should work towards processing the interferograms ourselves.

4.5.6 Ascending & Descending Orbits

We would like to explore if we can leverage the different geometries of ascending and descending orbits to better separate $\Delta\phi_{snow}$ from $\Delta\phi_{deformation}$.

4.5.7 ΔSWE Time Series Analysis

Carry out a time series analysis of interferograms from the beginning to the end of the accumulation season in order to recover absolute SWE in addition to ΔSWE over time.

4.6 Outlook

We will continue to explore improvements to our method. If it works, this method would refine measurements of ΔSWE for glaciers and therefore improve our understanding of the spatial and temporal distribution of ΔSWE throughout the accumulation season. This improved understanding of ΔSWE on glaciers could also lead to a better constrained glacier mass balance.

References

Conde, V., Mateus, P., Catalao, J., & Gritsevich, M. (2019, March). On the Estimation of Temporal Changes of Snow Water Equivalent by Spaceborne SAR Interferometry: A New Application for the Sentinel-1 Mission. *Journal of Hydrology and Hydromechanics*, *67*, 93–100. doi: 10.2478/johh-2018-0003

Deeb, E. (2012). *Estimating snow water equivalent (SWE) using interferometric synthetic aperture radar (InSAR) - ProQuest.* Retrieved 2020-10-14, from `http://www.proquest.com/docview/1268757228`

Gardner, A. S., Fahnestock, M. A., & Scambos, T. A. (2019). *ITS_live Regional Glacier and Ice Sheet Surface Velocities.* Retrieved 2020-12-19, from `https://its-live.jpl.nasa.gov/`

Guneriussen, T., Hogda, K. A., Johnsen, H., & Lauknes, I. (2001, October). InSAR for estimation of changes in snow water equivalent of dry snow. *IEEE Transactions on Geoscience and Remote Sensing*, *39*(10), 2101–2108. (Conference Name: IEEE Transactions on Geoscience and Remote Sensing) doi: 10.1109/36.957273

Krimmel, R. M. (2001). *Water, ice, meteorological, and speed measurements at South Cascade Glacier, Washington, 1999 balance year* (Report No. 2000-4265). Retrieved from `http://pubs.er.usgs.gov/publication/wri004265` (Edition: -) doi: 10.3133/wri004265

Leinss, S., Wiesmann, A., Lemmetyinen, J., & Hajnsek, I. (2015, August). Snow Water Equivalent of Dry Snow Measured by Differential Interferometry. *IEEE Journal of Selected Topics in Applied Earth Observations and Remote Sensing*, *8*(8), 3773–3790. (Conference Name: IEEE Journal of Selected Topics in Applied Earth Observations and Remote Sensing) doi: 10.1109/JSTARS.2015.2432031

Majumdar, S. (2019). *SNOW DEPTH AND SWE ESTIMATION USING SPACEBORNE POLARIMETRIC AND INTERFEROMETRIC SYNTHETIC APERTURE RADAR].*

Robinson, D. A., Dewey, K. F., & Heim, R. R. (1993). Global snow cover monitoring: An update. *Bulletin of the American Meteorological Society*, *74*(9), 1689 - 1696. Retrieved from `https://journals.ametsoc.org/view/journals/bams/74/9/1520-0477_1993_074_1689_gscmau_2_0_co_2.xml` doi: 10.1175/1520-0477(1993)074⟨1689:GSCMAU⟩2.0.CO;2

Rott, H., Nagler, T., & Scheiber, R. (2003, December). SNOW MASS RETRIEVAL BY MEANS OF SAR INTERFEROMETRY. *Proc. of FRINGE 2003 Workshop*, 6.

Tedesco, M., Derksen, C., Deems, J. S., & Foster, J. L. (2015). Remote sensing of snow depth and snow water equivalent. In *Remote sensing of the cryosphere* (p. 73-98). John Wiley Sons, Ltd. Retrieved from `https://onlinelibrary.wiley.com/doi/abs/10.1002/9781118368909.ch5` doi: https://doi.org/10.1002/9781118368909.ch5